Visualization of High Angular Resolution Diffusion MRI Data with Color-Coded LIC-Maps

M. Höller[1], F. Thiel[1], K.-M. Otto[1], U. Klose[2], H.-H. Ehricke[1]

[1]Institute for Applied Computer Science
Stralsund University of Applied Sciences
Zur Schwedenschnaze 15
18435 Stralsund
Mark.Hoeller@fh-stralsund.de
and
[2] MR Research Group
Dptm. of Diagnostic and Interventional Neuroradiology
University Hospital Tübingen
Hoppe-Sailer-Str. 3
72076 Tübingen
Uwe.Klose@med.uni-tuebingen.de

Abstract: In diffusion MRI a voxel's local diffusion profile may be visualized in detail by glyph-based techniques, e.g. ellipsoidal or superquadric tensor glyphs. Global representations, such as streamlines and streamtubes, provide fiber continuity, but may lead to misinterpretations due to deficiences of the tractography algorithm used. Line integral convolution (LIC) has been applied to diffusion tensors in order to bridge the gap between local and global representations. Recently, High Angular Diffusion Imaging (HARDI) techniques, such as Q-Ball Imaging (QBI), have been introduced into the clinical routine, bearing the potential of better resolving complex white matter configurations, e.g. crossing, branching and kissing fibers. In this paper we propose an extension of the LIC method to multi-directional vector fields, taking into account not only a single direction, but multiple directions of anisotropic diffusion of two or more fiber pathways passing through a voxel. For this purpose a multiple-kernel approach is presented and evaluated. We apply a color coding scheme for directional encoding of LIC slices, allowing better fiber continuity perception. Our results with simulation datasets and QBI data from a healthy volunteer emphasize the method's capability of easing the analysis of complex fiber architectures.

1 Introduction

In neuroimaging, since the advent of diffusion MRI the visualization of the anisotropic behavior of water molecules within white matter has become an area of constant research. Due to the complexity of fiber architectures, the reconstruction of fiber patways is a difficult task, particularly in regions of crossing, branching and kissing fibers. With Diffusion Tensor Imaging (DTI) the local diffusion profile is modelled by an ellipsoidal tensor with

three eigenvectors and corresponding eigenvalues. Approximately 30 percent of white matter voxels contain more than a single fiber pathway and thus multiple anisotropy directions [BBJ+07]. For these the tensor model is not adequate, since it cannot reliably resolve multiple directions.
With High Angular Resolution Imaging (HARDI) techniques a voxel's diffusion profile is acquired with a large number of gradient directions, thus providing a better angular resolution. In Q-Ball Imaging (QBI) typically more than 32 gradient directions are applied and the diffusion profile is described by reconstructing an Orientation Distribution Function (ODF) [Tuc04]. A variety of approaches have been proposed on ODF analysis in order to find relevant anisotropy directions, which may be used for tractography [TCC07, BBJ+07, SS08] . It has been demonstrated, that ODF sharpening approaches such as regularization [EOK11, SCPS05] , spherical deconvolution [TCGC04, DDKA09] or alternative reconstruction schemes [ALS+10] can improve tracking through regions of crossing and branching fiber pathways. In datasets acquired under clinical conditions with low b-values and signal to noise ratios (SNR) fiber crossing angles beyond 40 degrees cannot reliably be resolved [OEKK11]. For this reason visualization approaches, which utilize tractography algorithms in order to generate geometric representations of fibers, e.g. streamlines or streamtubes, are prone to errors and misinterpretations. On the other hand, glyph based visualizations, which present local diffusion profiles by e.g. Q-Ball glyphs, ellipsoids or superquadrics, lack fiber continuity and therefore miss to provide fiber connectivity information.
With texture based visualization methods the gap between representing local or global diffusion features may be bridged. Line integral convolution (LIC) techniques [Cab93] have been applied to DTI datasets, utilizing the tensor's main eigenvector to guide the construction of the filter kernel and the smooting process [WvdLH05, ZP03]. The result may be visualized by an arbitrary slice through the volume or in 3D by direct volume rendering of the LIC result [HA04]. Due to low contrast of the LIC result, the method has not widely been used for diffusion MRI visualization.
In this paper we propose a color coding approach for LIC slices, taking into account regional anisotropic diffusion directions and general fractional anisotropy (GFA) values. This allows us to substantially enhance image contrast and provide viewers of LIC slices with directional information. In order to better visualize regions of crossing and branching fibers, we extend the LIC algorithm to HARDI datasets, where the ODF represents a diffusion profile with potentially more than a single anisotropic diffusion direction.

2 Related work

In diffusion MRI various visualization methods have been introduced in the last decade, most of which focus on DTI. They may be categorized by (1) direct color mapping, (2) glyph based representations, (3) fiber geometries and (4) texture based methods.

In category 1, color-coded FA maps combine the voxel's fractional anisotropy (FA) with the color-coded prinicipal eigenvector direction of the diffusion tensor. The most widely

used scheme to date in which the components of the eigenvector (x, y, z) are assigned to the color channels red, green and blue was introduced by Pajevic and Pierpaoli [PP00]. From color-coded slice images the major pathways may be mentally reconstructed by grasping the orientation of the fiber in one voxel and following a path of similar color from one voxel to the next.

In category 2, different types of glyphs have been used in order to visualize the diffusion tensor's characteristics, e.g. diffusion direction and magnitude. The ellipsoid was the first glyph to be applied to DTI data by Pierpaoli and Basser [Pie96]. The shape of the diffusion ellipsoid depends on the diffusion anisotropy and is determined by the three eigenvalues and corresponding eigenvectors. Other glyphs, based on geometric primitives like cuboids and cylinders, were also proposed. Glyphs may be color-coded according to the principal eigenvector [TRW+02, TRWW03]. Kindlmann [Kin04] introduced superquadric glyphs, which combined symmetry properties of ellipsoids with the shape and orientation of cuboids and cylinders. This may ease the distinction between different shapes of the local diffusion profile. Kindlmann and Westin [KW06] proposed a method where the glyphs are no longer distributed over a regular grid. Instead, they calculate potential energies between neighboring tensors and place glyphs in a dense packing of the field. Glyph packing may be applied either to a slice or to the volume dataset as a whole. Glyphs can give the full tensor information for each voxel, whereas the geometry of pathways and thus connectivity information are difficult to perceive. Merging ellipsoids [ZCT09] is a visualization technique which aims at combining local tensor information with global connectivity features. For the visualization of HARDI datasets ODF glyphs my be used. They are constructed by deformation of a sphere surface according to ODF values distributed over a half sphere. Directional color-coding of ODF glyphs helps to reveal local anisotropy directions.

In category 3, results of tractography algorithms may be visualized by geometric objects using streamlines [MCCvZ99], streamtubes [ZDL03], hyperstreamlines [DH93] or tensorlines [WKL99]. The geometries clearly reveal the connection between brain regions, but fail to reliably show uncertainties due to problems of data acquisition and processing. They represent interpretations of the data and depend on processing parameters, e.g. choice of seed regions, tracking algorithms or termination criteria. This is also true for results of feature extraction methods [Sch09], which generate a pathway's complex hull e.g. by segmentation or fiber clustering [EN05, MVvW05, HJM+06, MMB+09].

Category 4 approaches employ textures in order to reveal relevant features of the vector field. Kindlmann et al. use the tensor volume to simulate a reaction-diffusion process of two chemicals in an anisotropic medium in order to produce a texture of spots, distributed over a non-regular grid [KWH00]. Feng et al. construct a set of non-overlapping ellipses as an input to a generalized anisotropic Lloyd relaxation process, resulting in textures similar to those generated by the reaction diffusion approach [FHHJ08]. LIC, which originally was proposed by Cabral and Leedom [Cab93], smoothes an input noise image with a vector field, using a convolution kernel, which is locally adapted by vector field integration.

McGraw et al. applied the LIC algorithm to a smoothed field of principal eigenvectors in order to visualize rat spinal cords [MVW+02]. Hsu was one of the first to apply LIC to a diffusion tensor field, using the tensor's principal eigenvector to guide the construction of a fixed-length filter kernel [Hsu01]. When using LIC the choice of the input noise texture strongly influences the resulting image. Kiu and Banks [BK96] use a multi-frequency input noise to visualize flow magnitude as well as it's direction. By changing the density, spot size and color intensity of the input image Hotz et al. [HFHH04] encode the eigenvalues of a positive-definite metric, that has the same topological structure as the tensor field. Wünsche et al. [WvdLH05] propose to create a three-dimensional LIC volume and visualize it by direct volume rendering. HyperLIC [ZP03] is a multipass approach, where the LIC algorithm is applied to the principal eigenvector, using a noise texture as input image to create an intermediate image. In the second pass the intermediate image from the previous pass is the input image for the application of LIC to the second eigenvector. The resulting image shows a global representation of the vector field. It is also possible to compute one LIC-image for every eigenvector and overlay the resulting images to get a fabric-like texture [HFHH04].

3 Method

3.1 Data preparation

We evaluate our methods with synthetic datasets from simulation studies. Moreover, in-vivo diffusion data from a healthy volunteer is used.

3.1.1 Synthetic data

Synthetic diffusion datasets were generated using a partial volume model similar to the one described in [BBJ+07]. We choose a diffusivity = 0.0015 mm^2/s, a baseline signal S_0 = 100 and a gradiant b-value of 2000 s/mm^2. We used a free volume fraction of 0.35 in voxels completely occupied by fiber segments. We generated datasets containing multimodal voxels with 5 mm fibers crossing at different angles and added noise to end up with a SNR = 0.35.

3.1.2 In vivo data

The diffusion data from the brain of a healthy 29 year old human female was aquired on a 3-T Trio MR scanner (Siemens Healtcare, Erlangen) using a spin-echo echo-planar diffusion-weighted sequence (TR = 8000 ms, TE = 105 ms) with 64 diffusion-encoding gradients, a b-value of 2000 s/mm^2 and an isotropic resolution of 2 mm. A data matrix of 108 x 108 was obtained measuring 56 slices.

3.1.3 Data preprocessing

We used a mutual information based retrospective motion correction scheme for the in vivo diffusion data in order to remove small motion that occured during the scan. For the simulated and the in vivo dataset we computed the diffusion tensor for each voxel and additionally reconstructed the ODF using Spherical Harmonics (SH) of order 8, enabling Laplace-Beltrami regularization and using a set of 606 ODF reconstruction directions evenly distributed on a hemisphere. The ODFs were sharpened by regularization using the approach described in [OEKK11]. We determined one or two main directions for each voxel by detecting the local maxima of the ODF. A second direction is valid when its minimum-to-maximum normalized ODF value reaches at least 15 per cent of the primary maximum's value. Moreover, we calculate fractional anisotropy (FA) volumes from the tensor data or generalized fractional anisotropy (GFA) volumes from the HARDI data.

3.2 Contrast enhanced LIC

We apply the LIC algorithm to the volume dataset, rather than to 2D slices with projected anisotropy directions. A 3D input noise volume is created by randomly distributing grey values from an 8 bit greyscale map. We use different resolution levels with resolutions usually higher than those of the original tensor or ODF fields. To each voxel of the input noise volume line integral convolution is applied with a box filter and a maximum length L of 12 integration steps for each direction. The stepsize is chosen as half the voxel size of the noise dataset. We use trilinear interpolation for computing direction vectors and FA/GFA values for each sample within the diffusion datasets. A FA/GFA threshold of 0.05 is used as a termination criterion for the tracking algorithm. Processing of the tensor datasets is carried out applying an Euler Integration on the principal eigenvectors. Further we compute a resulting vector $\vec{v}_R$ as a sum of all vectors $\vec{v}(P_i)$ along the streamline tracked.

$$\vec{v}_R = \sum_{i=-L}^{L} \vec{v}(P_i)$$

The vector is normalized to create a vector $\vec{v}_{RN}$ which will be used for directional color coding (see next chapter).

The resulting LIC greyscale volume may be visualized by computing 2D slice images (see Figure 1a) or by direct volume rendering. In order to enhance the contrast between background and fiber structures, the FA/GFA values are used. The grey values of the LIC texture may be weighted with the corresponding FA/GFA value, e.g. by mixing the two values at a ratio of 0.7 to 0.3 (Figure 1b). As an alternative, we propose to use the FA/GFA volumes as input for the LIC algorithm. In this approach we substitute the random noise volumes by noisy FA/GFA volumes, which are derived from the original data by adding random noise (Figure 1c). We experimented with different noise levels and achieved good results by adding random noise to the original grey values with a fraction of 25 percent.

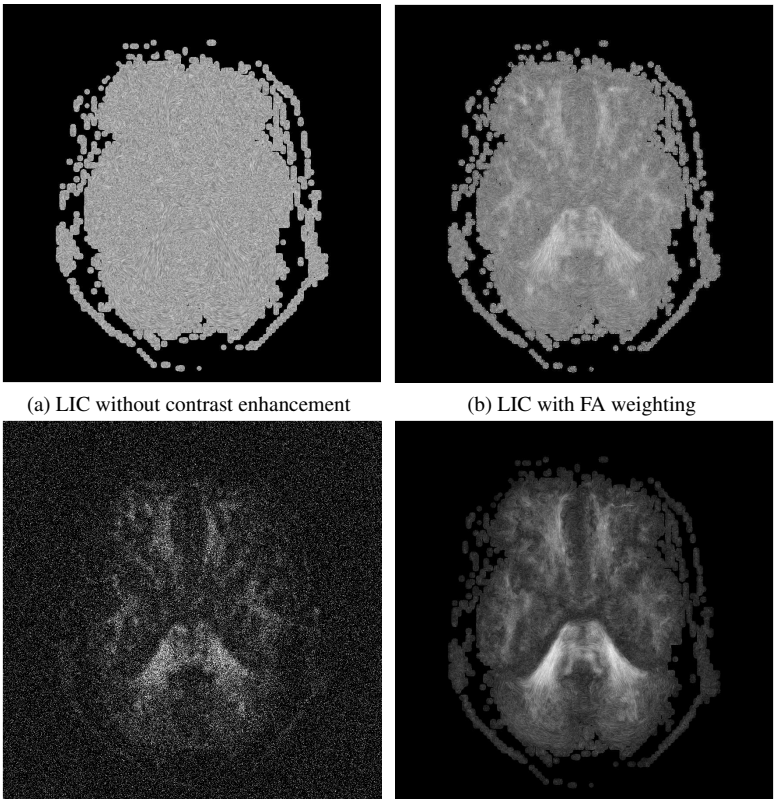

(a) LIC without contrast enhancement (b) LIC with FA weighting

(c) Noisy FA image (d) LIC using the noisy FA as input

Figure 1: An axial slice through the superior cerebellar peduncle from the in-vivo dataset: a) LIC result using white noise as input, b) contrast enhanced by weighting the LIC result from (a) with the FA volume, c) noisy FA image, d) LIC result using the noisy FA (c) as input.

Figure 1d demonstrates, that by this method the contrast between relevant fiber structures and background may substantially be enhanced.

3.3 Multiple direction 3D LIC

It is well known that the tensor model is not well suited for situations, where a voxel contains more than a single anisotropy direction. Consequently, with LIC approaches, that compute smoothing kernels by integration of the principal eigenvector field, branching, crossing or kissing fiber pathways cannot be reliably visualized. With the model-free ODF the local diffusion process can be represented with more detail. If more than a single

anisotropy direction is detected by ODF analysis, the LIC algorithm must be adapted so that it can use this information. We achieve this with a multiple-kernel approach. Applying multiple kernels means that for each sample we first analyze the ODF and determine its local maxima as explained above. In a first step we integrate along the main direction, which is the direction with the global maximum of ODF values. This way we construct a first smoothing kernel. If there is a second local ODF maximum we perform an integration along this second direction, thus producing a second smoothing kernel. Both kernels are used for noise smoothing. Only the first kernel is used for computing an average direction vector, which is used for directional color coding.
The method may be generalized to more than two directions, if these can reliably be detected.

3.4 Color coding

In DTI visualization color encoding schemes have widely been used to reveal multiple features of the datasets. Wünsche et al. [WL04] propose Anisotropy Modulated LIC, where in a first step the LIC texture is color mapped with diffusion anisotropy and in a second step the result is blended with the color mapped mean diffusitivity. Kindlmann et al. use barycentric opacity maps to assign an opacity to a voxel according to it's inherent type of diffusion [KWH00]. This allows the transparency of brain regions to be defined during volume rendering. They also use barycentric color maps to steer the lighting of the diffusion tensor.

We use the hue-saturation-brightness (HSB) color model to encode different diffusion properties. HSB is a color representation with a cone shaped color space. The hue channel is represented by rotation angles with an cone's main axis as rotation axis, reaching from red (0/360) over green (120) to blue (240). The saturation channel is encoded as fractional distance from the cone's center (0) to it's surface (100). Brightness is measured from black (0) to white (100) from the cone's basis to it's tip. Color coding is performed in order to depict different features of the LIC result.

In our color coding scheme we only use two channels of the HSB model. The saturation channel is always set to 100. The brightness is defined by the LIC value, which is generated as output of the noise smooting process. For directional encoding we use the direction of the vector $\vec{v}_{RN}$, representing the average anisotropic diffusion direction along the integrated directions. Our experiments with the application of the standard color coding scheme for FA maps [PP00], in which the volume axes x, y, z are encoded as red, green and blue of the RGB colormodel, yielded not-convincing results. In the resulting LIC image fiber continuity perception is blocked by abrupt color changes, due to changes in anisotropic diffusion direction (Figure 3a). We found that fiber continuity perception is enhanced by a color coding approach, in which fibers running parallel or nearly parallel to the current slice image possess similiar hues. Fibers with directions approximately orthogonal to the slice, are encoded with different hue values, allowing viewers to distinguish between in-plane and out-of-plane fibers (Figure. 3b).
In our approach the hue value is determined by the angle γ between the vector $\vec{v}_{RN}$ of the

voxel and a vector $\vec{r}$ orthogonal to the slice. The hue is computed by:

$$hue = 120 + 120 * \left(\frac{90° - \gamma}{90°} \right)$$

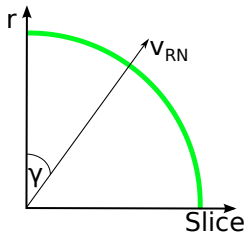

Figure 2: Definition of the color depending on the angle

When γ is 90°, the vector $\vec{v}_{RN}$ is located within the slice and we set hue to 120 (green). When the vector is orthogonal to the slice, γ is 0° and we set hue to 240 (blue), which results in a good contrast (Figure 2).

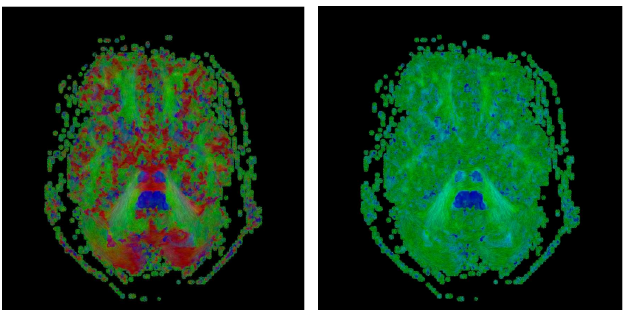

(a) LIC color coded with standard RGB

(b) LIC color coded with HSB color coding

Figure 3: Comparison of color coding methods of an axial slice through superior cerebellar peduncle from a proband study: a) using the standard RGB color coding method creates discontiniuties in fibers within the slice b) using our HSB method with two colors.

The processing and visualisation was performed on a Linux (Ubuntu 10.10) workstation with the following specifications: Intel Core i7-820QM (8MB cache, 1.74 GHz x 8 cores with hyperthreading), 16 GB RAM (DDR3, 1333 MHz), NVIDIA Quadro FX 880M (with 1GByte memory) graphics card. We used an in-house software written in Java.

4 Results

The approaches presented above were evaluated with synthetic datasets from simulation studies as well as in-vivo data from a healthy volunteer. We applied the multiple-kernel LIC method with directional HSB color-coding to visualize the superior cerebellar peduncle from the in vivo dataset. We studied the impact of different spatial resolutions of the input noise volume on the visualization of an axial slice image. Figure 4 shows the LIC result with an input noise texture with a resolution of 0.5 mm per pixel (4a) and 0.125 mm per pixel (4b). The calculation of one color-coded LIC slice with a resolution of 0.5 mm is done in 7 seconds. With a resolution of 0.125 mm the calculation took 113 seconds. These values can be improved significantly by using Fast-LIC [HS97]. It becomes obvious that using a higher resolution may better reveal the fibrous structures in the image. However, since computation time increases with better resolution, tradeoffs have to be made. We achieved good results with a resolution of 0.5 mm.

Furthermore, we used synthetic datasets to study how usage of the ODF with one or two

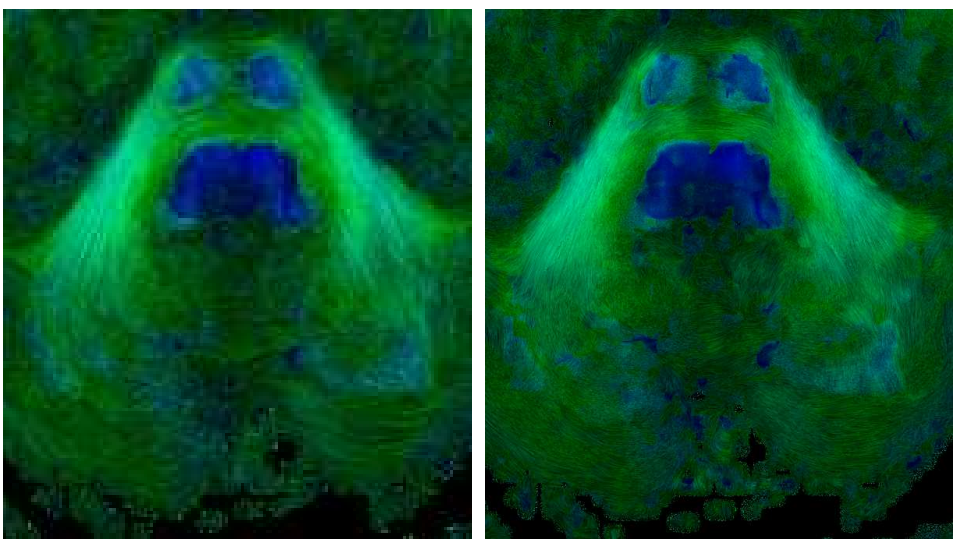

(a) resolution 0.5 mm (b) resolution 0.125 mm

Figure 4: Axial slices through brainstem and cerebellum comparing different resolutions of the noise input texture a) 0.5 mm per pixel, b) 0.125 mm per pixel.

diffusion maxima may influence the visualization of complex fiber architectures. We used an input noise texture with an isotropic voxel size of 0.125 mm and applied LIC to the principal eigenvector of the diffusion tensor (Figure 5a). With respect to the ODF dataset, we calculated an image using the direction of the global maximum (Figure 5b) as well as an image applying the multiple-kernel method to two anisotropic diffusion directions, if available (Figure 5c). We also used the HSB color coding method. All anisotropic diffusion directions of the crossing pathways (crossing angle 55 degrees) are located within the

slice, thus being represented with green color. It can be seen that by usage of the tensor or the ODF with only one diffusion maximum (Figure 5a,5b) the crossing can not be visualized adequately. Instead, the tensor approach implies two kissing fibers. Applying the ODF with only one direction better resolves the crossing situation, whereas usage of the multiple-kernel approach correctly delineates the crossing structure.

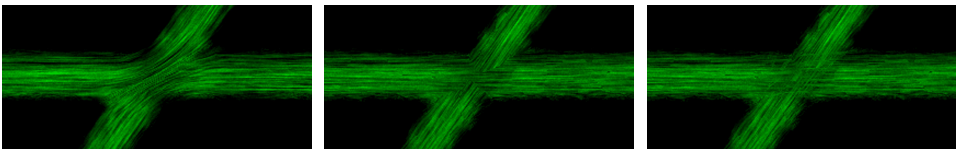

(a) LIC using Tensor

(b) LIC using one local maximum of ODF

(c) LIC using a multiple-direction kernel

Figure 5: Comparison of using one (a,b) and two (c) anisotropic diffusion directions of a synthetic dataset with two fibers crossing at an angle of 55 degrees. a) shows LIC using the diffusion tensor, b) using one direction of the regularized ODF and c) using a two direction filter Kernel on the basis of the regularized ODF. All results are color coded with the HSB model.

In an in-vivo experiment we applied Gaussian noise to the the FA volume and used it as input noise texture. We computed a color coded LIC volume and chose a coronal slice through the cortico-spinal tract (Figure 6). We applied the HSB color-coding scheme to the resulting slice. The figure demonstrates that with LIC it becomes possible to visualize fiber pathways with good continuity without the need for setting seed points.

5 Discussion

In this paper we presented an extension of the LIC algorithm for the visualization of HARDI datasets from diffusion MRI. The application of LIC may close the gap between local and global visualization techniques, which dominate diffusion MRI analysis. Our approach allows more than a single anisotropy direction within a sample to be taken into account. With simulation studies we could demonstrate the method's benefit for the analysis of fiber crossing situations. Our results show, that with a multiple direction LIC algorithm misinterpretations with respect to kissing and crossing fibers may be avoided. The question, whether these preliminary results can be reproduced with clinical studies is still open and needs further study. We could further demonstrate that by usage of noisy FA/GFA volumes as input for the LIC algorithm, the contrast between fiber pathways and background structures could be enhanced. In our opinion our color coding model for LIC slice images allowed better perception of fiber continuity. The amendments to the LIC approach, presented in this paper, may help to strengthen the impact of LIC on radiological diagnosis and make it a valuable method for diffusion MRI analysis.

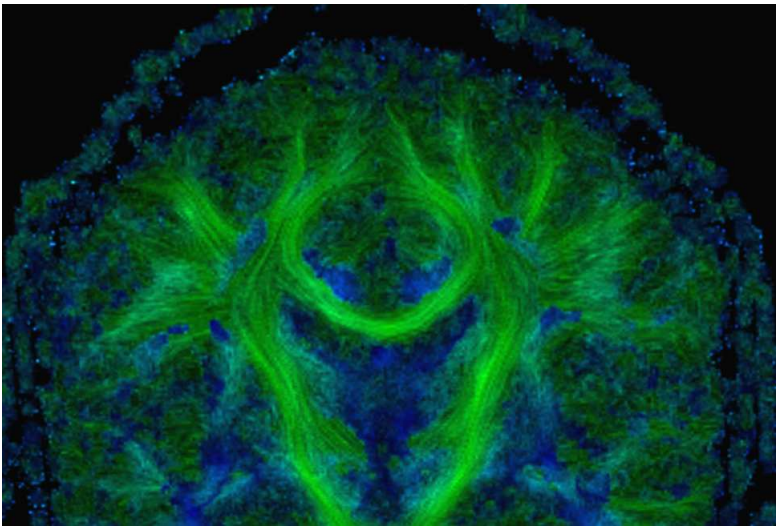

Figure 6: Color-coded LIC slice through the cortico-spinal tract using a noisy FA texture as input.

References

[ALS+10] Iman Aganj, Christophe Lenglet, Guillermo Sapiro, Essa Yacoub, Kamil Ugurbil, and Noam Harel. Reconstruction of the orientation distribution function in single- and multiple-shell q-ball imaging within constant solid angle. *Magn Reson Med*, 64(2):554–566, August 2010.

[BBJ+07] T E J Behrens, H Johansen Berg, S Jbabdi, M F S Rushworth, and M W Woolrich. Probabilistic diffusion tractography with multiple fibre orientations: What can we gain? *Neuroimage*, 34(1):144–155, January 2007.

[BK96] David C Banks and Ming-Hoe Kiu. Multi-Frequency Noise for LIC. *Proceedings of the 7th conference on Visualization '96*, (Lic), 1996.

[Cab93] Brian Cabral. Imaging vector fields using line integral convolution. *Proceedings of the 20th annual conference on*, 1993.

[DDKA09] Maxime Descoteaux, Rachid Deriche, Thomas R Knösche, and Alfred Anwander. Deterministic and probabilistic tractography based on complex fibre orientation distributions. *IEEE Trans Med Imaging*, 28(2):269–286, February 2009.

[DH93] Thierty Delmarcelle and L Hesselink. Visualizing second-order tensor fields with hyperstreamlines. *IEEE Computer Graphics and Applications*, 13(4):25–33, 1993.

[EN05] Frank Enders and Christopher Nimsky. Visualization of White Matter Tracts with Wrapped Streamlines. In *Visualization, 2005. VIS 05. IEEE*, pages 51 – 58, 2005.

[EOK11] Hans-H Ehricke, Kay-M Otto, and Uwe Klose. Regularization of bending and crossing white matter fibers in MRI Q-ball fields. *Magnetic Resonance Imaging*, 29(7):916–926, 2011.

[FHHJ08] Louis Feng, Ingrid Hotz, Bernd Hamann, and Kenneth Joy. Anisotropic noise samples. *IEEE transactions on visualization and computer graphics*, 14(2):342–54, 2008.

[HA04] Anders Helgeland and Oyvind Andreassen. Visualization of vector fields using seed LIC and volume rendering. *IEEE transactions on visualization and computer graphics*, 10(6):673–82, 2004.

[HFHH04] Ingrid Hotz, Louis Feng, Hans Hagen, and Bernd Hamann. Physically based methods for tensor field visualization. *Visualization, 2004.*, 2004.

[HJM+06] Patric Hagmann, Lisa Jonasson, Philippe Maeder, Jean-Philippe Thiran, Van J Wedeen, and Reto Meuli. Understanding diffusion {MR} imaging techniques: from scalar diffusion-weighted imaging to diffusion tensor imaging and beyond. *Radiographics*, 26 Suppl 1:205–223, 2006.

[HS97] HC Hege and D Stalling. Fast LIC with Higher Order Filter Kernels. *MATHEMATICAL VISUALIZATION*, 74(December), 1997.

[Hsu01] E Hsu. Generalized line integral convolution rendering of diffusion tensor fields. *Proceedings of the International Society for Magnetic*, 9:98425, 2001.

[Kin04] Gordon Kindlmann. Superquadric Tensor Glyphs. 2004.

[KW06] Gordon Kindlmann and Carl-Fredrik Westin. Diffusion tensor visualization with glyph packing. *IEEE transactions on visualization and computer graphics*, 12(5):1329–35, 2006.

[KWH00] Gordon Kindlmann, David Weinstein, and David Hart. Strategies for Direct Volume Rendering of Diffusion Tensor Fields. *IEEE Trans Vis Comput Graph*, 6(2):124–138, 2000.

[MCCvZ99] S Mori, B J Crain, V P Chacko, and P C van Zijl. Three-dimensional tracking of axonal projections in the brain by magnetic resonance imaging. *Ann Neurol*, 45(2):265–269, February 1999.

[MMB+09] Dorit Merhof, Martin Meister, Ezgi Bingol, Christopher Nimsky, and Günther Greiner. Isosurface-based generation of hulls encompassing neuronal pathways. *Stereotactic and functional neurosurgery*, 87(1):50–60, January 2009.

[MVvW05] B. Moberts, A. Vilanova, and J.J. van Wijk. Evaluation of Fiber Clustering Methods for Diffusion Tensor Imaging. *IEEE Visualization 2005 - (VIS'05)*, pages 9–9, 2005.

[MVW+02] T Mcgraw, B C Vemuri, Z Wang, Y Chen, M Rao, and T Mareci. Line Integral Convolution for Visualization of Fiber Tract Maps from DTI. *Computer*, pages 615–622, 2002.

[OEKK11] Kay Otto, Hans-Heino Ehricke, Vinod Kumar, and Uwe Klose. Angular smoothing and radial regularization of ODF fields: Application on deterministic crossing fiber tractography. *Physica Medica*, In Press, 2011.

[Pie96] Carlo Pierpaoli. Toward a quantitative assessment of diffusion anisotropy. *Magnetic resonance in medicine*, 1996.

[PP00] S Pajevic and C Pierpaoli. Color schemes to represent the orientation of anisotropic tissues from diffusion tensor data: application to white matter fiber tract mapping in the human brain. *Magnetic resonance in medicine : official journal of the Society of Magnetic Resonance in Medicine / Society of Magnetic Resonance in Medicine*, 43(6):921, June 2000.

[Sch09] Thomas Schultz. Feature Extraction for DW-MRI Visualization: The State of the Art and Beyond â. In *Proc. Dagstuhl Scientific Visualization Workshop*, 2009.

[SCPS05] Peter Savadjiev, Jennifer S W Campbell, G Bruce Pike, and Kaleem Siddiqi. {3D} curve inference for diffusion {MRI} regularization. *Med Image Comput Comput Assist Interv Int Conf Med Image Comput Comput Assist Interv*, 8(Pt 1):123–130, 2005.

[SS08] Thomas Schultz and Hans-Peter Seidel. Estimating crossing fibers: a tensor decomposition approach. *IEEE Trans Vis Comput Graph*, 14(6):1635–1642, 2008.

[TCC07] J-Donald Tournier, Fernando Calamante, and Alan Connelly. Robust determination of the fibre orientation distribution in diffusion {MRI}: non-negativity constrained super-resolved spherical deconvolution. *Neuroimage*, 35(4):1459–1472, 2007.

[TCGC04] J-Donald Tournier, Fernando Calamante, David G Gadian, and Alan Connelly. Direct estimation of the fiber orientation density function from diffusion-weighted {MRI} data using spherical deconvolution. *Neuroimage*, 23(3):1176–1185, November 2004.

[TRW+02] David S Tuch, Timothy G Reese, Mette R Wiegell, Nikos Makris, John W Belliveau, and Van J Wedeen. High angular resolution diffusion imaging reveals intravoxel white matter fiber heterogeneity. *Magn Reson Med*, 48(4):577–582, 2002.

[TRWW03] David S Tuch, Timothy G Reese, Mette R Wiegell, and Van J Wedeen. Diffusion {MRI} of complex neural architecture. *Neuron*, 40(5):885–895, 2003.

[Tuc04] David S Tuch. Q-ball imaging. *Magn Reson Med*, 52(6):1358–1372, 2004.

[WKL99] David Weinstein, Gordon Kindlmann, and Eric Lundberg. Tensorlines: advection-diffusion based propagation through diffusion tensor fields. In *VIS '99: Proceedings of the conference on Visualization '99*, pages 249–253, Los Alamitos, CA, USA, 1999. IEEE Computer Society Press.

[WL04] Burkhard Wünsche and Richard Lobb. The 3d visualization of brain anatomy from diffusion-weighted magnetic resonance imaging data. *of the 2nd international conference on*, 2004.

[WvdLH05] Burkhard Wünsche, Jarno van der Linden, and Nathan Holmberg. DTI volume rendering techniques for visualising the brain anatomy. *International Congress Series*, 1281(0):80 – 85, 2005. ¡ce:title¿CARS 2005: Computer Assisted Radiology and Surgery¡/ce:title¿ ¡xocs:full-name¿Proceedings of the 19th International Congress and Exhibition¡/xocs:full-name¿.

[ZCT09] Song Zhang, Stephen Correia, and David F. Tate. Visualizing diffusion tensor imaging data with merging ellipsoids. *2009 IEEE Pacific Visualization Symposium*, pages 145–151, April 2009.

[ZDL03] S Zhang, C Demiralp, and D H Laidlaw. Visualizing diffusion tensor mr images using streamtubes and streamsurfaces. *IEEE Transactions on Visualization and Computer Graphics*, 9(4):454–462, 2003.

[ZP03] Xiaoqiang Zheng and Alex Pang. HyperLIC. *Visualization, 2003. VIS 2003. IEEE*, 2003.